THE JOURNAL OF BIOLOGICAL CHEMISTRY
Vol. 278, No. 27, Issue of July 4, pp. 24825–24830, 2003
Printed in U.S.A.

Crystal Structure of Neisserial Surface Protein A (NspA), a Conserved Outer Membrane Protein with Vaccine Potential*

Received for publication, March 19, 2003, and in revised form, April 24, 2003
Published, JBC Papers in Press, April 26, 2003, DOI 10.1074/jbc.M302803200

Lucy Vandeputte-Rutten‡, Martine P. Bos§¶, Jan Tommassen§, and Piet Gros‡‖

From the ‡Department of Crystal and Structural Chemistry, Bijvoet Center for Biomolecular Research and the §Department of Molecular Microbiology, Institute of Biomembranes, Utrecht University, Padualaan 8, 3584 CH Utrecht, The Netherlands

The neisserial surface protein A (NspA) from *Neisseria meningitidis* is a promising vaccine candidate because it is highly conserved among meningococcal strains and induces bactericidal antibodies. NspA is a homolog of the Opa proteins, which mediate adhesion to host cells. Here, we present the crystal structure of NspA, determined to 2.55-Å resolution. NspA forms an eight-stranded antiparallel β-barrel. The four loops at the extracellular side of the NspA molecule form a long cleft, which contains mainly hydrophobic residues and harbors a detergent molecule, suggesting that the protein might function in the binding of hydrophobic ligands, such as lipids. In addition, the structure provides a starting point for structure-based vaccine design.

The Gram-negative bacterium *Neisseria meningitidis* causes life-threatening meningitis and septicaemia in humans. Based on the immunological characteristics of the capsular polysaccharides, *N. meningitidis* strains are divided in 12 serogroups. Strains of serogroups A, B, and C are the predominant cause of meningococcal disease (1). Effective vaccines, which consist of capsular polysaccharide conjugated to tetanus toxoid protein to generate sufficient immunological memory, are now available against serogroups A and C (2, 3). Unfortunately however, the capsular polysaccharide of serogroup B is poorly immunogenic, making this type of vaccine ineffective (4, 5). Therefore, attention has shifted toward the possibility of using outer membrane proteins (OMPs)[1] as targets for vaccine development (6). OMPs perform a variety of functions including the following: (*a*) they may form channels in the outer membrane for uptake of nutrients or the secretion of proteins; (*b*) they may be enzymes involved in, for example, the modification of lipopolysaccharides or in proteolysis; or (*c*) they may function as adhesins mediating the interaction of the bacterium to host cells. Despite these different functions, they appear to share a common fold, *i.e.* they form trans-membrane β-barrels consisting of antiparallel amphipathic β-strands. The number of β-strands in the OMPs, of which the structure has been solved, varies and ranges from 8 to 22 (7). The best-studied OMPs for vaccine development against *N. meningitidis* are the porins PorA and PorB and the adhesin OpcA, which elicit bactericidal and protective antibody responses (8). However, due to the antigenic heterogeneity of these proteins (9) or phase-variable expression of their genes (10), they are unable to provide protection against all or most of the serogroup B strains. Recently, the 18-kDa OMP NspA (Neisserial surface protein A) has been identified (11), which is remarkably conserved among *N. meningitidis* and *Neisseria gonorrhoeae* isolates (11–15). The function of NspA is unknown, but it shows considerable sequence similarity with members of the Opa family of OMPs (11), which are important adhesins involved in the entry of neisseriae into epithelial cells by interacting, for example, with the human carcinoembryonic antigen cell adhesion molecule (CEACAM) receptors (16, 17). Several studies have shown that NspA can elicit antibodies that are protective and bactericidal against a wide range of *N. meningitidis* serogroup B strains, making NspA an attractive vaccine candidate (11–15). Recently, Moe *et al.* (18) showed that sequential immunization using vesicles derived from different meningococcal strains, thus containing different PorA, PorB, and lipopolysaccharide types, resulted in a protective antibody response against NspA, underscoring the importance of NspA as a possible vaccine candidate.

To date, the crystal structure of only one OMP of *N. meningitidis* has been solved, *i.e.* that of OpcA (19), which forms a closed 10-stranded β-barrel. Structural studies can not only provide insight into the function of OMPs, but they can also reveal the conformation of epitopes that are recognized by bactericidal antibodies, thus being helpful for the design of vaccines. Here, we describe the crystal structure of NspA, at 2.55-Å resolution, which shows an eight-stranded antiparallel β-barrel structure with a hydrophobic groove at the extracellular side harboring a detergent molecule.

EXPERIMENTAL PROCEDURES

Cloning of the nspA Gene and Expression of the Recombinant Protein—Genomic DNA of *N. meningitidis* strain H44/76 was prepared using the Qiagen genomic preparation kit. The part of the *nspA* gene encoding the mature domain of the protein, *i.e.* without the 19-amino acid signal peptide, was PCR-amplified with the primer pair 5′-gctacatatggaaggcgcatccggcttttacg-3′ and 5′-gctaggatcctcagaatttgacgcgcacaccgg-3′. The PCR product was cloned into pCRII-TOPO (Invitrogen), digested with *Nde*I and *Bam*HI, and ligated into pET11a (Novagen), yielding pET11a-NspA. Five-liter cultures of *Escherichia coli* strain BL21(DE3) (Novagen), containing pET11a-NspA, were grown at 37 °C in L-broth (20) containing 100 μg/ml ampicillin. At an optical density at 600 nm of 0.6, 0.1 mM of isopropyl-thio-β-D-galactopyranoside was added to induce expression of the recombinant gene. After another 4 h

* This work was supported by the council for Chemical Sciences of the Netherlands Organization for Scientific Research (NWO-CW). The costs of publication of this article were defrayed in part by the payment of page charges. This article must therefore be hereby marked "*advertisement*" in accordance with 18 U.S.C. Section 1734 solely to indicate this fact.

The atomic coordinates and structure factors (code 1P4T) have been deposited in the Protein Data Bank, Research Collaboratory for Structural Bioinformatics, Rutgers University, New Brunswick, NJ (http://www.rcsb.org/).

¶ Supported by the European Community project MenB vaccine QLRT-1999-CT-00359.

‖ To whom correspondence should be addressed. Tel.: 31-30-2533502; Fax: 31-30-2533940; E-mail: p.gros@chem.uu.nl.

[1] The abbreviations used are: OMP, outer membrane protein; OMV, outer membrane vesicle; NspA, neisserial surface protein A; DodMe2NprSO3, 3-dimethyldodecylammoniopropane-sulfonate; O-POE, *n*-octyl-poly-oxyethylene.

TABLE I
Summary of data and refinement statistics

	Native	$KAu(CN)_2$
Data set statistics		
Resolution limits (outer shell) (Å)	40–2.55 (2.64–2.55)	40–3.95 (4.09–3.95)
Space group	R32	R32
Unit cell parameters (Å,°)	$a = 97.37$, $b = 97.37$, $c = 171.94$, $\alpha = 90$, $\beta = 90$, $\gamma = 120$	$a = 97.83$, $b = 97.83$, $c = 171.87$, $\alpha = 90$, $\beta = 90$, $\gamma = 120$
Mosaicity (°)	0.319	0.492
Oscillation range (°)/total oscillation (°)	1/125	1/370
Total no. of reflections (outer shell)	125,566 (8944)	98,783 (3304)
No. of unique reflections (outer shell) [a]	10,350 (1029)	5388 (549)
R_{merge} (%) (outer shell) [b]	7.0 (37.5)	5.0 (12.2)
Completeness (%) (outer shell)	98.6 (99.7)	99.9 (100)
$I/\sigma(I)$ (outer shell)	19.0 (5.2)	23.5 (16.7)
Refinement statistics		
Resolution range (Å)	30–2.55	
Total no. of non-hydrogen atoms	1278	
R_{work} (%)	22.2	
R_{free} (%)	25.8	
r.m.s.d. [c] bond lengths (Å)	0.016	
r.m.s.d. bond angles (°)	1.77	

[a] For the $KAu(CN)_2$ data set, the Friedel mates have been counted separately.
[b] $R_{merge} = \Sigma (I - \langle I \rangle) / \Sigma (I)$.
[c] r.m.s.d., root-mean-square deviation.

of incubation at 37 °C, cells were harvested and washed with 600 ml of 0.9% (w/v) NaCl. NspA was present in inclusion bodies, which were isolated according to Dekker *et al.* (21) and solubilized in 8 M urea containing 10 mM glycine, pH 8.0. Residual insoluble material and membranes were removed by ultracentrifugation (100,000 $g \times$ for 1 h).

Refolding and Purification of NspA—Urea-solubilized NspA protein was folded *in vitro* by 5-fold dilution into 20 mM ethanolamine, pH 11, containing 1% (w/v) 3-dimethyldodecylammoniopropane-sulfonate (DodMe2NprSO3, Fluka) and left overnight at room temperature while stirring. Refolding was evaluated by SDS-PAGE on gels containing 14% acrylamide under "seminative" conditions, *i.e.* with no SDS in the gel and only 0.03% instead of 3% SDS in the 3-fold sample buffer (additionally containing 0.1 M Tris-HCl, pH 6.8, 15.4% (v/v) glycerol, 7.7% (v/v) β-mercaptoethanol, and 0.008% (w/v) bromphenol blue) and without heating before electrophoresis. For denaturation, the sample was boiled for 5 min with 1% (w/v) SDS. The gels were stained with Coomassie Brilliant Blue for visualization of the protein bands. To purify the folded NspA, the mixture was loaded onto a 1-ml mono S column (Amersham Biosciences), pre-equilibrated with 10 mM DodMe2NprSO3, 20 mM Tris-HCl, pH 8.5 (buffer A). Prior to loading, the pH of the protein sample was adjusted to pH 8.5 using 1 M HCl. The column was washed with buffer A, and proteins were eluted with a linear gradient of 0–500 mM NaCl in buffer A, total volume 50 ml. Fractions containing folded NspA were pooled, diluted 10-fold in buffer A, and again loaded on a mono S column. The column was washed with buffer B (20 mM Tris-HCl, pH 7.5, 0.06% (v/v) *n*-decylpentaoxyethylene ($C_{10}E_5$; Bachem P-1005)). The protein was eluted with 500 mM NaCl in buffer B and concentrated to 6 mg/ml using Centricon concentrators with molecular mass cutoff of 10 kDa (Amicon). The protein was dialyzed three times against 10 ml of 0.06% $C_{10}E_5$ prior to crystallization.

Chemical Cross-linking—A 200-μl sample of NspA was incubated at 0.2 mg/ml in 20 mM buffer (either sodium acetate, pH 4.5, or Tris-HCl, pH 8.5) containing 1% (v/v) *n*-octyl-poly-oxyethylene (O-POE, Alexis), and 5 μl of a 1% stock solution of glutaraldehyde in 1% (v/v) O-POE was added. The cross-linking reaction was allowed to proceed for 4 h at room temperature. Subsequently, 100 μl of SDS-PAGE sample buffer was added, and 20 μl of this solution was analyzed by SDS-PAGE.

Analytical Ultracentrifugation—Protein molecular weights were determined by sedimentation equilibrium centrifugation experiments, using a Beckman Optima XL-A analytical Ultracentrifuge with absorbance monitoring. Cells contained double-sector charcoal-filled epon centerpieces and had column lengths of ~8 mm and depths of 3 mm. A protein sample of 50 μl was used. The sedimentation equilibrium experiments were run at 18,000 rpm at 20 °C using a loading concentration of ~1.0 mg/ml corresponding to a measured absorption at 280 nm (A_{280}) of ~0.3 in the cell. Optima XL-A data analysis software running under the program Microcal Origin version 3.78 (MicroCal Software, Inc.) was used to calculate the molecular weight. Data were fitted to single component and monomer/dimer models. A density of 1 g/cm^3 was assumed for the solvent plus detergent, which was 1% (v/v) O-POE and 20 mM Tris-HCl, pH 8.5.

Crystallization of NspA and Data Collection—NspA at a concentration of 6 mg/ml in 0.06% (w/v) $C_{10}E_5$ was crystallized at 4 °C by the hanging drop vapor diffusion method against a reservoir solution of 12% (w/v) polyethylene glycol 3000 , 0.1 M lithium sulfate, 0.1 M *N*-(2-acetamido)iminodiacetic acid (Fluka), pH 6.6, and 2% (v/v) isopropanol. The crystallization drops contained equal volumes (0.5 μl) of reservoir solution and purified NspA. Crystals were hexagonal and grew to a size of up to 0.5 × 0.5 × 0.1 mm^3 in a few days. Crystals were soaked in a cryo solution containing the reservoir solution, 0.06% (w/v) $C_{10}E_5$, and 20% (v/v) glycerol and directly cooled in liquid nitrogen. X-ray data were collected at 100 K on a charge-coupled device (CCD) detector at the ID14 EH1 beamline at the European Synchrotron Radiation Facility (ESRF). Native data were collected to 2.55-Å resolution using a wavelength of 0.933 Å and an oscillation range of 1°. The space group of the crystal was R32 (for the native data set, $a = b = 97.37$ Å, $c = 171.94$ Å in the trigonal setting). Due to the position of the crystal in the loop, which caused the long 3-fold axis to be perpendicular to the plane of the loop, we measured over 125° to obtain a complete data set. This resulted in a high redundancy of ~9. Derivative data were collected at 100 K on the EMBL beamline X11 at DESY (Hamburg). The wavelength was 0.811 Å. Crystals contained one monomer in the asymmetric unit and had a V_m of 4.74 Å^3/Da, corresponding to a solvent plus detergent content of 74% (v/v). All diffraction data were processed using DENZO (22), SCALEPACK (22), and TRUNCATE (23).

Heavy Atom Derivatives and Phasing—The structure was finally solved using the single-wavelength anomalous dispersion phasing method. Initially, molecular replacement was tried because NspA shares sequence similarity with OmpA and, to a lesser extent, with OmpX. The core β-barrel of OmpA (Protein Data Bank code 1qjp) was used for molecular replacement. Most residues were replaced by alanines. The structure could not be refined properly, and therefore, a heavy atom derivative was prepared. A crystal was soaked for 1 h in 2 μl of reservoir solution containing 0.06% $C_{10}E_5$ and 10 mM of the heavy atom compound. Anomalous signals were calculated using SCALEPACK. The $KAu(CN)_2$ data set showed the highest anomalous signal with a total χ^2 of 4.5 (10 in the lowest resolution shell and 1.5 in the highest resolution shell). For convenience and due to the presence of ice rings, the data were processed to only 3.95-Å resolution. Shake and Bake (DREAR/SnB package) (24) was used to find the gold atom positions. Two sites were found; one $Au(CN)_2^-$ was close (~3 Å) to Phe-27, which is located close to the trimer axis. The distances between three gold peaks was ~6.8 Å. The second peak was found close to the backbone of Ser-144. Phases were subsequently calculated using MLPHARE (23) to 4.0-Å resolution. This yielded an R-cullis of 0.79. With density modification in CNS (25), phases were extended to 2.55-Å resolution using the native data set. Model building was performed using the program O (26), and the structure was refined using simulated annealing and individual *B*-factor refinement using REFMAC5 (27).

RESULTS

Refolding and Quaternary Structure of NspA—NspA was overproduced without its signal sequence in *E. coli*, which resulted in the formation of NspA protein aggregates (inclusion bodies). After solubilization of these inclusion bodies, NspA was refolded in a buffer containing the detergent DodMe2NprSO3. Folding was monitored by seminative SDS-PAGE. OMPs are generally heat-modifiable, *i.e.* folded monomers run faster in SDS-PAGE gels than heat-denatured proteins. In contrast, we observed that NspA migrated slower in the gel after refolding. The denatured protein migrated at a mass of ~18 kDa, whereas the folded protein migrated at 22 kDa, which agrees well with the electrophoretic mobility of native NspA isolated from neisserial membranes (14). To investigate whether the reduced electrophoretic mobility of folded NspA is due to dimerization, we performed analytical ultracentrifugation experiments as well as chemical cross-linking. Both methods (data not shown) as well as the crystal structure (see below) strongly indicated that NspA is a monomer in a detergent-containing solution.

Structure Solution—The NspA structure was solved with the single-wavelength anomalous dispersion phasing method using $KAu(CN)_2$. The refined model contained one monomer (155 amino acids), five partial $C_{10}E_5$ molecules, one sulfate ion, one ethanolamine, and nine water molecules in the asymmetric unit and had a crystallographic R-factor of 22.2% and an R_{free} of 25.8% for data in the 30–2.55-Å resolution range. For the side chains Glu-1, Lys-53, and Lys-79, no electron density was observed, and therefore these were omitted from the Protein Data Bank file. The Ramachandran plot shows 92.4% of the φ/ψ combinations in the most favored regions, 6.1% in the additionally allowed regions, and 0.8% (residue Asn-38 and Thr-138, which are present in T1 and L4, respectively) in the disallowed regions. The overall temperature factor is 40 $Å^2$. Table I summarizes the statistics of the crystallographic data and refinement. The crystal packing consisted of crystallographic trimers, which were packed in alternating directions in such a way that the upper part of the molecule that faced up made contacts with the upper part of a symmetry-related molecule that faced down.

Overall Structure—NspA (Fig. 1*A*) consists of an eight-stranded antiparallel β-barrel with a height of ~50 Å and a main chain diameter of ~20 Å. It has a shear number of 10 with β-strands having an angle of ~40° with respect to the barrel axis. In general, OMPs contain short turns at the periplasmic side of the protein and longer loops at the extracellular side with the N and C termini located at the periplasmic side (see, for example, Refs. 19, 30, and 31). The four long loops of NspA are therefore likely to be located at the extracellular side of the membrane. Like other OMPs, NspA contains two rings of aromatic residues (Fig. 1*A*) that flank both sides of the membrane and may stabilize the position of the barrel in the membrane (32). The lower ring contains 7 aromatic residues, whereas the upper ring is less well defined. Located on top of the upper aromatic ring is a rim of mainly basic residues that contains 7 lysines and 3 arginines (Fig. 1*B*), a feature also found in other OMPs (33). Four detergent ($C_{10}E_5$) molecules are present at the sides of the barrel (Fig. 1*A*). Two of them are present at the interfaces of the crystallographic trimer, which indicates that NspA is probably not a trimer in solution. The inside of the β-barrel harbors an extensive hydrogen-bonding network as well as cavities, but there is no pore through which ions or other molecules could be transported. The periplasmic side of NspA is mainly basic in the center with 5 positively charged residues residing in the middle and some aspartates further away from the β-barrel axis (Fig. 2*A*). The four extracellular loops of NspA form a long groove at the top of the molecule, which is highly hydrophobic (Fig. 2*B*). Interestingly, we observed additional electron density at the location of this hydrophobic groove, in the $2F_o - F_c$ and $F_o - F_c$ omit-electron density maps of NspA, which probably corresponds to part of a $C_{10}E_5$ detergent molecule (Fig. 2*C*).

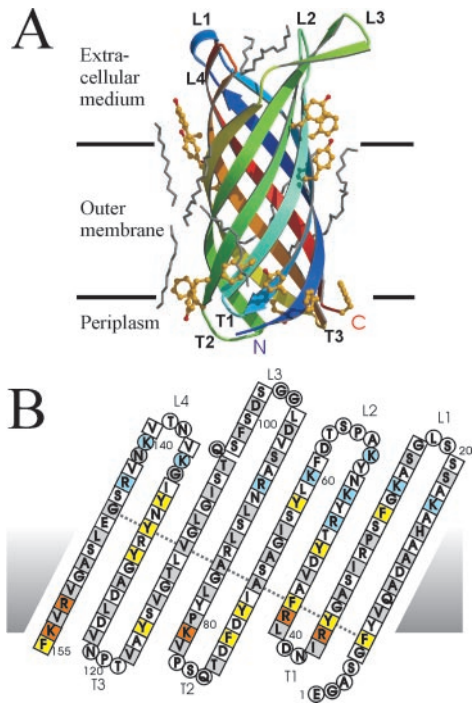

FIG. 1. **Overall structure of NspA.** *A*, a ribbon representation of NspA with the N terminus in *blue* and the C terminus in *red* and the color gradient in between. Aromatic residues located at the membrane boundaries are drawn in *ball-and-stick* model in *yellow* with the oxygen atoms in *red*. Parts of the $C_{10}E_5$ molecules for which electron density was observed are shown in *gray bonds*. In the figure, no distinction is made between the carbon and oxygen atoms, and two of the $C_{10}E_5$ molecules shown are symmetry-related to others. Membrane boundaries are indicated by the *black lines*. *B*, topology plot of NspA. Amino acids are shown with one-letter codes. Residues present in β-strands are shown as *squares*. Other residues are presented as *circles*. Aromatic residues residing in the two rings flanking the membrane are colored *yellow*. Basic residues that form a basic rim on top of the upper aromatic ring are presented in *blue*, and those that are at the bottom in the middle of the β-barrel are colored *orange*. Side chains of residues that are shaded *gray*, *yellow*, or *blue* point to the outside of the barrel. Extracellular loops are labeled *L1* to *L4*, and the periplasmic turns are labeled *T1* to *T3*. The *dashed line* indicates the hydrogen-bonding register within the β-barrel. *Panel A* from this figure and from Figs. 2*C* and 3 were prepared using Bobscript (28) and Raster3D (29).

Loop Structures—NspA contains four long extracellular loops, which are well conserved among the different neisserial strains. The loops have relatively low temperature factors, allowing for accurate determination of their conformations. Loops 2 and 4 show some uncommon features when compared with the more standard β-hairpin loops seen in β-sheet structures. In the case of loop 2, this could be the result of crystal contacts with the same loop from five other symmetry-related NspA molecules (Fig. 3*A*). However, the presence of a conformation-restraining proline in the middle of the extremity of the loop might indicate that loop 2 indeed has an uncommon conformation in the native NspA structure. In loop 4, adjacent residues, Gly-134 and Lys-135 in strand 7 and Lys-140 and Asn-141 in strand 8, are directed outwards from the barrel. Loops 1 and 3 both adopt a 2:4 tight β-hairpin conformation. Loop 3 (Fig. 3*A*) contains 2 glycine residues, which have a large degree of freedom for backbone angles, at its extremity. The conformation of the loop seems to be stabilized by a hydrogen

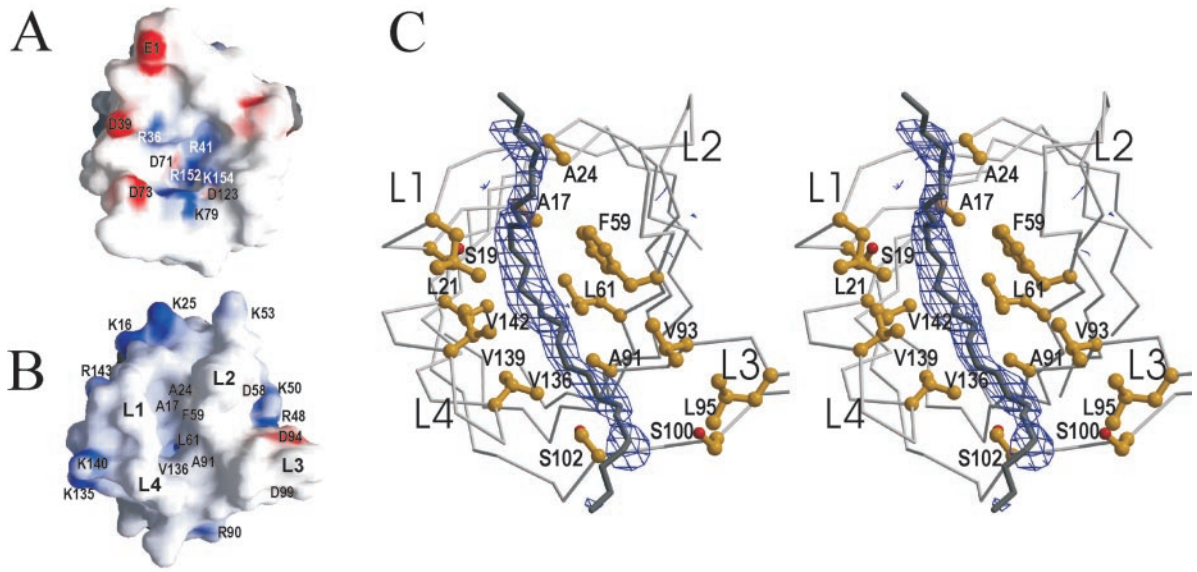

FIG. 2. **NspA viewed from the periplasmic side and the extracellular side.** *A*, bottom view (periplasmic side), and *B*, top view (extracellular side), showing the electrostatic surface potentials. The surface is colored *blue* for potentials >10 *kT*/e and *red* for potentials <−10 *kT*/e. Loops are indicated with *L1* to *L4*. Some residue positions are indicated by the one-letter code. *C*, stereo representation of the NspA β-barrel as Cα trace, in *light gray*, viewed from the top. Residues that are within a distance of 4.5 Å to the detergent molecule in the crystal structure are shown in a *ball-and-stick* model and are labeled by the one-letter code. Carbon atoms are colored *yellow*, and oxygen atoms are colored *red*. A complete $C_{10}E_5$ detergent molecule is shown in *dark gray*, and the electron density observed in the $2F_o - F_c$ map is shown in *blue* around the detergent molecule, in which no distinction is made between oxygen and carbon atoms. Fig. 2, *A* and *B*, was prepared using GRASP (34).

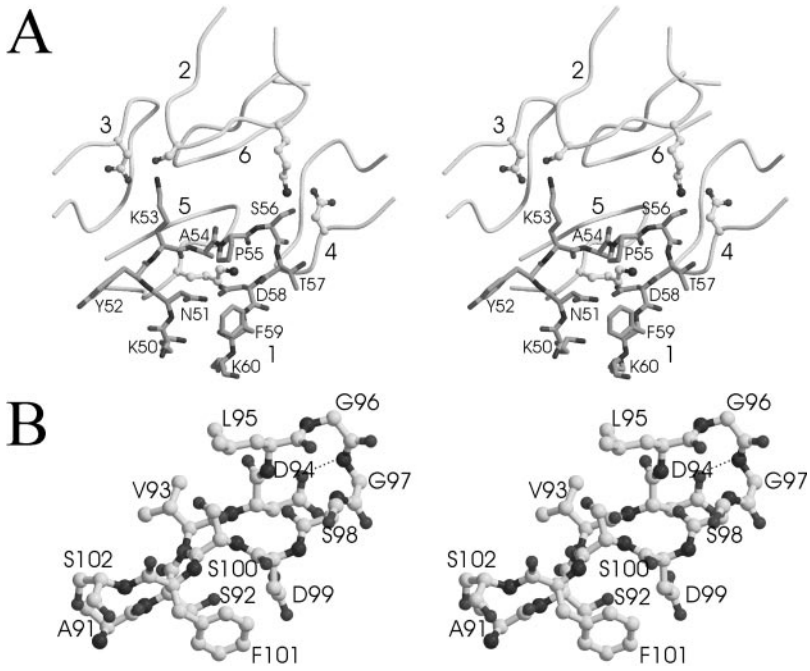

FIG. 3. **Structure of loops 2 and 3.** *A*, loop 2 in *gray sticks* and with labels shown together with five symmetry-related loop 2s, which are shown as *coils*. Residues in the symmetry-related loops (labeled *2*–*6*) that make hydrogen bonds to residues in the original (labeled *1*) are shown by a *ball-and-stick* model. *B*, stereo representation of a *ball-and-stick* model of a part of the immunodominant loop 3. Residues are labeled, and one of the hydrogen bonds is indicated by a *dotted line*.

bond between a side chain oxygen of Asp-94 and the backbone nitrogen of Gly-97. Due to the presence of two well exposed aspartates, Asp-94 and Asp-99, the loop is negatively charged. This is in contrast with the overall positive charge of NspA, which has a theoretical isoelectric point of 9.64.

Homology of NspA to Other Outer Membrane Proteins—Three other OMP structures that contain eight β-strands have been solved before, *i.e.* the crystal structures of OmpA (35) and OmpX (36) and the solution structure of PagP (37), all from *E. coli*. We searched for more structural homologs of NspA in the Protein Data Bank using the program DALI (38). This search revealed OmpA and OmpX with the highest z scores of 17.8 and 12.9, respectively, and 144 and 139 Cα atoms of NspA overlay with the Cα atoms of OmpA and OmpX with root-mean-square deviations of 2.5 and 3.4 Å, respectively. The structure of NspA resembles that of OmpA most, probably because the OmpA β-barrel also has a shear number of 10, whereas the shear number of OmpX is 8. The third protein found by the DALI search was a soluble bacterial protein, quinohemoprotein amine dehydrogenase from *Paracoccus denitrificans* (39), a part of which forms of an eight-stranded β-barrel. Using the DALI program, we also found that 126 Cα atoms of NspA can be superpositioned on OpcA (19), a 10-stranded β-barrel from *N. meningitidis*, with an root-mean-square deviation of only 3.0 Å and a z score of 9.3. Similarly, another 10-stranded β-barrel, OmpT from *E. coli* (31), superpositions on NspA with 122 residues with an root-mean-square deviation of 3.8 Å and a z score of 9.4. Although these scores reflect the overall similari-

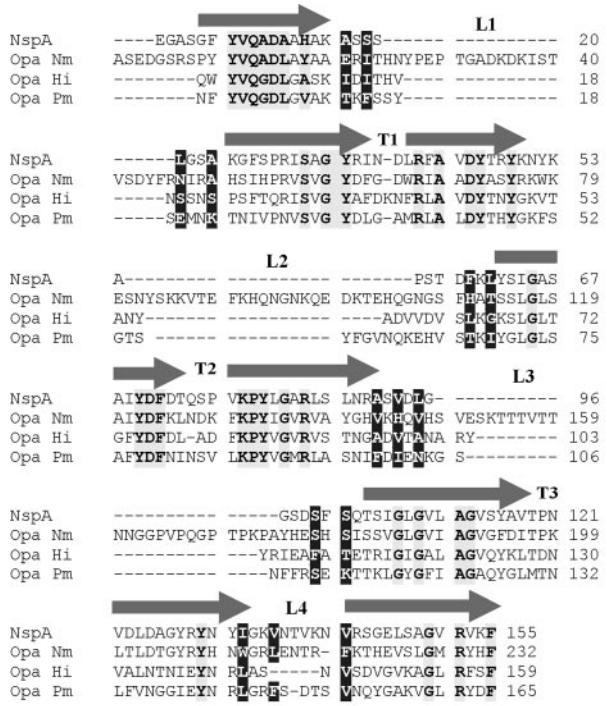

FIG. 4. **Sequence alignment.** Alignment of NspA from strain H44/76 with an Opa protein from *N. meningitidis* serogroup A strain B494 (Opa Nm, GenBank™ accession number AAC45976), with a homologous OMP from *H. influenzae* (Opa Hi, GenBank™ accession number AAC23104), and with an OMP from *P. multocida* (Opa Pm, GenBank™ accession number AAK03109). Fully conserved residues are shown with a *light gray background*. Residues that make contact to the detergent molecule in the groove at the top of NspA are shown in *white letters* with a *dark gray background*. *Arrows* indicate the β-strands in NspA.

ties between these 8- and 10-stranded β-barrels, no further remarkable similarities between NspA on the one hand and OpcA or OmpT on the other hand could be detected.

NspA shares the highest sequence homology (~38.7% identity) to the members of the neisserial Opa protein family of adhesins (Fig. 4). No three-dimensional structure has been solved for these important molecules, but Marlorny *et al.* (40) predicted the topology of Opa. Residues that are present in the membrane-spanning β-strands of NspA are highly conserved between NspA and Opa, particularly the residues that are located on the inside of the β-barrel. It is therefore likely that the structures of Opa and NspA are highly similar in the membrane-spanning region. A major difference between NspA and Opa is the length of the extracellular loops, which are much longer in Opa proteins. Using the sequence similarity between Opa and NspA, we refined the previously predicted Opa topology model (Fig. 4). In the previous topology model, turn 2 was exceptionally long. In the crystal structure of NspA, this turn is almost as short as the other two turns. Based on the sequence homology between Opa and NspA, it is likely that the fourth strand in the previously predicted topology model has to be shifted toward the extracellular side by 8 residues.

NspA has, in addition, high sequence similarity (~35% identity) with two non-characterized Opa proteins from *Haemophilus influenzae* and *Pasteurella multocida* (Fig. 4). The loops from the *H. influenzae* and *P. multocida* proteins are more comparable in length with the loops in NspA than with those of the neisserial Opa proteins. Since the hydrophobic groove harboring a detergent molecule is a remarkable feature of the NspA structure, we examined specifically whether the hydrophobic residues contacting the detergent molecule are conserved in the *H. influenzae* and *P. multocida* proteins. Although none of them was fully conserved, most of the substitutions involved replacements by other hydrophobic residues, especially in the cases of the residues that are located most centrally.

DISCUSSION

There is an obvious need for a vaccine that offers protection against diverse group B meningococcal strains. As described in the Introduction, this vaccine should consist of non-capsular components, such as the OMPs present in outer membrane vesicles (OMVs). The major hurdle in development of such a vaccine has been the fact that the meningococcus possesses a huge capacity to change its outer surface by phase and antigenic variation of many of its OMPs. For this reason, the OMV vaccines tested so far were very effective against their homologous strains but offered far less protection against heterologous strains. Therefore, novel vaccine candidates that are conserved among strains and will likely confer broad protection need to be identified. One very promising vaccine candidate is NspA, which is remarkably conserved among neisserial strains. The relatively low amount of NspA generally present in OMVs may prevent a sufficiently high immune response against this protein in vaccines. However, Moe *et al.* (18) have recently shown that sequential immunization with OMVs that were heterologous for the major immunodominant OMPs, but all contained NspA, resulted in protective immunity that was at least partly mediated by bactericidal anti-NspA antibodies. Thus, given in the correct formulation, NspA could be a very important novel vaccine component. Our present study aids in the further development of NspA-based vaccines. For example, we developed efficient procedures to produce NspA and to refold it *in vitro* into its native conformation. This refolded NspA can be used in vaccine formulations. As an alternative strategy, the use of peptide vaccines can be considered. In general, bactericidal antibodies are directed to conformational epitopes, which are, in OMPs, typically located in the extracellular loops. In a previous study, we described that bactericidal antibodies could not be elicited in mice with a linear peptide derived from an epitope from PorA. However, based on the crystal structure of a peptide containing a sequence derived from a PorA epitope in complex with a Fab fragment of a bactericidal antibody, a conformationally restrained peptide was designed. With this peptide, a specific bactericidal immune response could be elicited, demonstrating the value of structural information (41). In NspA, loop 3 is the longest of the four loops and is probably, as in the crystal structure, most exposed *in vivo*. Hou *et al.* (43) have shown that loop 3 is an important target for bactericidal antibodies directed against recombinant NspA. The structure of the extracellular loops, particularly loop 3, may greatly aid in the design of peptide vaccines.

The function of NspA is not known yet, although experiments performed by Moe *et al.* (15) suggest that NspA is at least not necessary for causing bacteremia in infant rats. Nevertheless, the observation that NspA is highly conserved and is expressed in all neisserial strains tested so far suggests that its function is important. Based on the sequence similarity of NspA to Opa proteins, which are adhesins facilitating colonization of the human naso-pharynx, it could be possible that NspA is an adhesin as well. However, preliminary experiments, in which we measured the adherence of an *E. coli* strain overexpressing NspA to primary human corneal cells, do not support this idea. Either NspA is not adhesin or its adhesive function is blocked on the surface of *E. coli*, possibly due to the long lipopolysaccharides. It is interesting that the structure of NspA contains a remarkable hydrophobic groove at the top of the molecule, which harbors a detergent molecule. Among the crystal structures of the closed OMPs, *i.e.* OmpA, OmpX, PagP,

OmpT, OpcA, and OMPLA (42), only OmpX also contains a central hydrophobic patch at the extracellular side of the molecule, but it does not form such an extended groove as in NspA. Possibly, NspA could bind a lipid-like molecule, such as a membrane lipid, *in vivo*, thereby possibly playing a role in the invasion of *N. meningitidis* into host cells by interacting with the lipid bilayer of these cells. Future studies, which can now be guided by the elucidated structure of NspA, will bring more insight into the function of NspA.

Acknowledgments—We are grateful for measurement time at beamline ID14-EH1 at the European Synchrotron Radiation facility (ESRF) in Grenoble, where the native data set has been measured. We also thank Andrea Schmith for helping at X11 at the European Molecular Biology Laboratory (EMBL) Outstation at Deutsches Elektronen Synchrotron (DESY) in Hamburg.

REFERENCES

1. Frasch, C. E. (1989) *Clin. Microbiol. Rev.* **2** (suppl.) S134–S138
2. Anderson, E. L., Bowers, T., Mink, C. M., Kennedy, D. J., Belshe, R. B., Harakeh, H., Pais, L., Holder, P., and Carlone, G. M. (1994) *Infect. Immun.* **62,** 3391–3395
3. Costantino, P., Viti, S., Podda, A., Velmonte, M. A., Nencioni, L., and Rappuoli, R. (1992) *Vaccine* **10,** 691–698
4. Zollinger, W. D., and Mandrell, R. E. (1983) *Infect. Immun.* **40,** 257–264
5. Mandrell, R. E., and Zollinger, W. D. (1982) *J. Immunol.* **129,** 2172–2178
6. Poolman, J., and Berthet, F. X. (2001) *Vaccine* **20,** Suppl. 1, S24–S26
7. Schulz, G. E. (2002) *Biochim. Biophys. Acta* **1565,** 308–317
8. Saukkonen, K., Abdillahi, H., Poolman, J. T., and Leinonen, M. (1987) *Microb. Pathog.* **3,** 261–267
9. Rosenqvist, E., Hoiby, E. A., Wedege, E., Caugant, D. A., Froholm, L. O., McGuinness, B. T., Brooks, J., Lambden, P. R., and Heckels, J. E. (1993) *Microb. Pathog.* **15,** 197–205
10. Rosenqvist, E., Hoiby, E. A., Wedege, E., Kusecek, B., and Achtman, M. (1993) *J. Infect. Dis.* **167,** 1065–1073
11. Martin, D., Cadieux, N., Hamel, J., and Brodeur, B. R. (1997) *J. Exp. Med.* **185,** 1173–1183
12. Plante, M., Cadieux, N., Rioux, C. R., Hamel, J., Brodeur, B. R., and Martin, D. (1999) *Infect. Immun.* **67,** 2855–2861
13. Cadieux, N., Plante, M., Rioux, C. R., Hamel, J., Brodeur, B. R., and Martin, D. (1999) *Infect. Immun.* **67,** 4955–4959
14. Moe, G. R., Tan, S., and Granoff, D. M. (1999) *Infect. Immun.* **67,** 5664–5675
15. Moe, G. R., Zuno-Mitchell, P., Lee, S. S., Lucas, A. H., and Granoff, D. M. (2001) *Infect. Immun.* **69,** 3762–3771
16. Virji, M., Makepeace, K., Ferguson, D. J., and Watt, S. M. (1996) *Mol. Microbiol.* **22,** 941–950
17. Chen, T., and Gotschlich, E. C. (1996) *Proc. Natl. Acad. Sci. U. S. A.* **93,** 14851–14856
18. Moe, G. R., Zuno-Mitchell, P., Hammond, S. N., and Granoff, D. M. (2002) *Infect. Immun.* **70,** 6021–6031
19. Prince, S. M., Achtman, M., and Derrick, J. P. (2002) *Proc. Natl. Acad. Sci. U. S. A.* **99,** 3417–3421
20. Tommassen, J., van Tol, H., and Lugtenberg, B. (1983) *EMBO J.* **2,** 1275–1279
21. Dekker, N., Merck, K., Tommassen, J., and Verheij, H. M. (1995) *Eur. J. Biochem.* **232,** 214–219
22. Otwinowski, Z., and Minor, W. (1997) *Methods Enzymol.* **276,** 307–326
23. Collaborative Computational Project, N. (1994) *Acta Crystallogr. Sect. D Biol. Crystallogr.* **50,** 760–763
24. Weeks, C. M., and Miller, R. (1999) *Acta Crystallogr. Sect. D Biol. Crystallogr.* **55,** 492–500
25. Brunger, A. T., Adams, P. D., Clore, G. M., DeLano, W. L., Gros, P., Grosse-Kunstleve, R. W., Jiang, J. S., Kuszewski, J., Nilges, M., Pannu, N. S., Read, R. J., Rice, L. M., Simonson, T., and Warren, G. L. (1998) *Acta Crystallogr. Sect. D Biol. Crystallogr.* **54,** 905–921
26. Jones, T. A., Zou, J. Y., Cowan, S. W., and Kjeldgaard (1991) *Acta Crystallogr. Sect. A* **47,** 110–119
27. Murshudov, G. N., Vagin, A. A., Lebedev, A., Wilson, K. S., and Dodson, E. J. (1999) *Acta Crystallogr. Sect. D Biol. Crystallogr.* **55,** 247–255
28. Esnouf, R. M. (1999) *Acta Crystallogr. Sect. D Biol. Crystallogr.* **55,** 938–940
29. Merrit, E. A., and Murphy, M. E. P. (1994) *Acta Crystallogr. Sect. D Biol. Crystallogr.* **50,** 869–873
30. Koronakis, V., Andersen, C., and Hughes, C. (2001) *Curr. Opin. Struct. Biol.* **11,** 403–407
31. Vandeputte-Rutten, L., Kramer, R. A., Kroon, J., Dekker, N., Egmond, M. R., and Gros, P. (2001) *EMBO J.* **20,** 5033–5039
32. Schulz, G. E. (2000) *Curr. Opin. Struct. Biol.* **10,** 443–447
33. Zeth, K., Diederichs, K., Welte, W., and Engelhardt, H. (2000) *Structure Fold Des.* **8,** 981–992
34. Nicholls, A., Sharp, K. A., and Honig, B. (1991) *Proteins* **11,** 281–296
35. Pautsch, A., and Schulz, G. E. (1998) *Nat. Struct. Biol.* **5,** 1013–1017
36. Vogt, J., and Schulz, G. E. (1999) *Structure Fold. Des.* **7,** 1301–1309
37. Hwang, P. M., Choy, W. Y., Lo, E. I., Chen, L., Forman-Kay, J. D., Raetz, C. R., Prive, G. G., Bishop, R. E., and Kay, L. E. (2002) *Proc. Natl. Acad. Sci. U. S. A.* **99,** 13560–13565
38. Holm, L., and Sander, C. (1993) *J. Mol. Biol.* **233,** 123–138
39. Datta, S., Mori, Y., Takagi, K., Kawaguchi, K., Chen, Z. W., Okajima, T., Kuroda, S., Ikeda, T., Kano, K., Tanizawa, K., and Mathews, F. S. (2001) *Proc. Natl. Acad. Sci. U. S. A.* **98,** 14268–14273
40. Malorny, B., Morelli, G., Kusecek, B., Kolberg, J., and Achtman, M. (1998) *J. Bacteriol.* **180,** 1323–1330
41. Oomen, C. J., Hoogerhout, P., Bonvin, A. M. J. J., Kuipers, B., Brugghe, H., Timmermans, H., Haseley, S. R., van Alphen, L., and Gros, P. (2003) *J. Mol. Biol.* **328,** 1083–1089
42. Snijder, H. J., and Dijkstra, B. W. (2000) *Biochim. Biophys. Acta* **1488,** 91–101
43. Hou, V. C., Raad, Z., Moe, G. R., Davé, A., and Granoff, D. M. (2002) *13th International Pathogenic Neisseria Conference, September 1–6, 2002*, p. 127 (abstr.), Norwegian Institute of Public Health, Oslo, Norway